ACS APPLIED MATERIALS & INTERFACES

Research Article

www.acsami.org

Highly Stable CO_2/N_2 and CO_2/CH_4 Selectivity in Hyper-Cross-Linked Heterocyclic Porous Polymers

Muhammad Saleh,[†,‡] Han Myoung Lee,[‡] K. Christian Kemp,[‡] and Kwang S. Kim*[,‡]

[†]Department of Chemistry, Pohang University of Science and Technology, Pohang 790-784, Korea

[‡]Department of Chemistry, Ulsan National Institute of Science and Technology (UNIST), Ulsan 689-798, Korea

Supporting Information

ABSTRACT: The largest obstacles for landfill/flue gas separation using microporous materials are small adsorption values and low selectivity ratios. This study demonstrates that these adsorption and selectivity challenges can be overcome by utilizing a series of hyper-cross-linked heterocyclic polymer networks. These microporous organic polymers (MOPs) were synthesized in a single step by inexpensive Friedel–Crafts-catalyzed reactions using dimethoxymethane as an external linker. The amorphous networks show moderate Brunauer–Emmett–Teller surface areas up to 1022 $m^2\ g^{-1}$, a narrow pore size distribution in the range from 6 to 8 Å, and high physicochemical stability. Owing to the presence of the heteroatomic pore surfaces in the networks, they exhibit maximum storage capacities for CO_2 of 11.4 wt % at 273 K and 1 atm. Additionally, remarkable selectivity ratios for CO_2 adsorption over N_2 (100) and CH_4 (15) at 273 K were obtained. More importantly, as compared with any other porous materials, much higher selectivity for CO_2/N_2 (80) and CO_2/CH_4 (15) was observed at 298 K, showing that these selectivity ratios remain high at elevated temperature. The very high CO_2/N_2 selectivity values are ascribed to the binding affinity of abundantly available electron-rich basic heteroatoms, high CO_2 isoteric heats of adsorption (49–38 kJ mol^{-1}), and the predominantly microporous nature of the MOPs. Binding energies calculated using the high level of ab initio theory showed that the selectivity is indeed attributed to the heteroatom–CO_2 interactions. By employing an easy and economical synthesis procedure these MOPs with high thermochemical stability are believed to be a promising candidate for selective CO_2 capture.

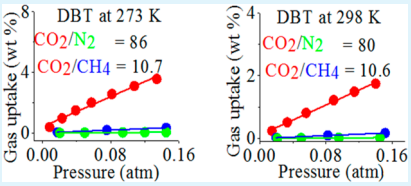

KEYWORDS: *Friedel–Crafts catalysis, microporous organic polymers, gas uptake, selectivity, carbon storage*

INTRODUCTION

Anthropogenic carbon dioxide (CO_2) and methane (CH_4) emissions are thought to be one major cause of global warming, and this issue has drawn worldwide attention due to its environmental solutions to prevent further global warming.[1,2] In recent years, new technologies/processes have been introduced for CO_2 capture, storage, and utilization.[1] Of these technologies, CO_2 capture is an approach that can be carried out before the situation gets too dire. Power plant flue gases contain about 75% N_2, 14% CO_2, and 10% moisture content; therefore, selective adsorption of CO_2 is a key issue to be taken into account while designing new polymers.[3,4] Additionally, selective CO_2 adsorption materials are important, as natural gas reserves contain, besides CH_4, roughly 40% CO_2 and N_2, which must be removed prior to combustion.[5] Therefore, separation of CO_2 from CH_4 is of equal importance for both academic and industrial applications. Aqueous amines such as ethanolamine have been widely used to adsorb CO_2, but the process for the regeneration of the amine and recovery of CO_2 is highly expensive.[6] A cheap alternative solution to this problem is physical sorption of CO_2 by porous solid materials, including porous zeolites,[7] metal–organic frameworks,[8] and microporous organic polymers.[9] In these porous polymer networks, saturation of CO_2 adsorption occurs at high pressure. However, in the low-pressure range, the CO_2 capacities are not high because of the lack of strong affinity toward the CO_2 molecule. Several strategies have been developed to increase the CO_2 storage capacity and the adsorption selectivity for CO_2 over N_2, i.e., increasing the isosteric heat of adsorption between sorbent and sorbate.[10] Similarly, by incorporating either CO_2-philic or N_2-phobic species in the polymeric framework, selectivity can be enhanced. So far, microporous organic polymers (MOPs) synthesized based on nitrogen-containing functional groups have good CO_2 adsorption capacity and selectivity at 273 K; however, the selectivity of these materials deteriorates rapidly at room temperature. Other functional groups containing heteroatoms of relatively close basic character to nitrogen like sulfur and oxygen have potential to increase or stabilize selectivity in an identical polymeric system at 298 K which is important for flue gas/fossil fuel thermal power plant applications. These heteroatoms can be introduced through inclusion of particular functionalities in the building units and postsynthetic modification. Recently, the introduction of nitrogen and phosphorus heteroatoms into MOPs has been shown to increase gas adsorption and selectivity.[11,12]

Porous organic materials are a rapidly growing field, which combines porous properties with organic functionalities.[5] Other materials in this category are metal organic frameworks

Received: February 3, 2014
Accepted: May 2, 2014
Published: May 2, 2014

   dx.doi.org/10.1021/am500728q | ACS Appl. Mater. Interfaces 2014, 6, 7325–7333

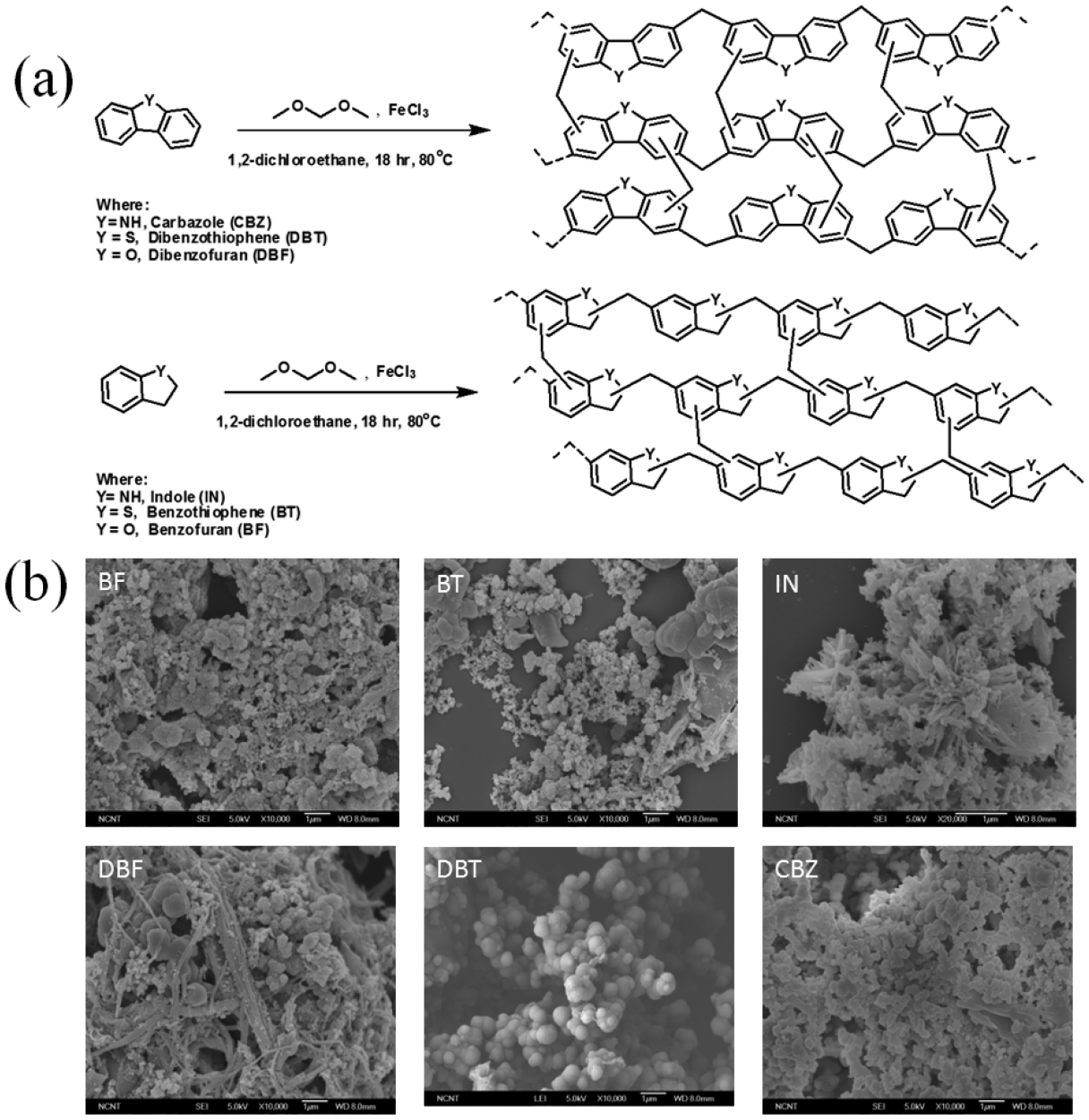

Figure 1. (a) Synthesis scheme of aromatic heterocyclic microporous polymers and (b) their FESEM images (at 1 μm scale).

(MOFs),[5] covalent organic frameworks (COFs),[13] porous organic cages,[14] carbon-based materials,[15] and microporous organic polymers (MOPs),[16] etc. MOPs are of particular interest due to their significantly unique properties such as large surface area, low skeletal density, and high thermal/chemical stability.[17] Second, these materials adsorb gases through physical adsorption, which results in a lowering of the regeneration cost. Hyper-cross-linking is one of the successful methods developed that facilitates high inner surface area in combination with significant pore volume in MOPs.[18] This hyper-cross-linking can be introduced in the polymers either by extensive cross-linking of polymer chains in an expanded state or by bottom-up assembling of rigid aromatic building units. In either of these approaches, the structure of the material does not collapse even after the removal of the solvent as the numerous rigid cross-linking sites permanently develop the porosity. For these reasons, MOPs are good candidates for applications like gas storage, gas separations, and catalysis. These materials have been extensively studied for H_2 and CH_4 storage; however, few reports detail the CO_2 adsorption properties of hyper-cross-linked MOPs.

To meet the challenges of carbon capture and storage technologies, sorbents with high gas uptake, high selective adsorption, good thermochemical stability, and low cost are desired. Most MOPs are synthesized by the reactions which are catalyzed by transition metal catalysts or noble metal catalysts, which has increased their capital cost and limited their practical applications.[19,20] MOPs having hyper-cross-linking can be prepared using different routes like oxidative polymerization of thiophenes,[21] cross-linking of organolithium compounds,[22] and cross-linking of polyaniline or polypyrrole.[23,24] However, the MOPs obtained by Friedel−Crafts (FC) alkylation catalyzed by Lewis acids ($FeCl_3$) are important for gas storage applications as this method provides a cost-effective single-step route for synthesis of MOPs in bulk scale.

dx.doi.org/10.1021/am500728q | ACS Appl. Mater. Interfaces 2014, 6, 7325−7333

Herein, we introduce a series of novel nanoporous hyper-cross-linked polymer networks which are obtained through FC cross-linking between dimethoxymethane (DMM) and a number of rigid nonfunctionalized heteroatomic aromatic building blocks (Figure 1a). To the best of our knowledge, this is the first study exploring the adsorption properties of CO_2 and CH_4 in combination with selective adsorption of CO_2 over N_2 and CH_4 by using heterocyclic microporous polymers at both temperatures of 273 and 298 K. These polymers are significantly less expensive, with respect to the price of monomers and catalysts, than other materials prepared by rare metal catalyzed coupling reactions. The synthesized microporous networks have a specific surface area of 1022 $m^2 g^{-1}$ and exhibit highly stable selectivity for CO_2 adsorption over CH_4 and N_2 at both 273 and 298 K. Theoretical calculations together with experimental analysis show important changes in the electronic density of the heteroatomic aromatic systems, which in turn affects the adsorption potential for CO_2 depending on the nature of the hyper-cross-linked systems.

EXPERIMENTAL SECTION

General Methods. X-ray diffraction (XRD) patterns were recorded from 5 to 40° on a Riguka, Japan, RINT 2500 V X-ray diffractometer using Cu Kα irradiation (λ = 1.5406 Å). Fourier transformed infrared (FTIR) spectra were recorded in KBr pellets using a Bruker FTIR. Field emission scanning electron microscopy (FESEM) images of the product were taken on a field emission scanning electron microscope (FESEM, JEOL, FEG-XL 30S) operating at an accelerating voltage of 5.0 kV. An energy-dispersive X-ray (EDX) detector was used to analyze the chemical elements of the samples operating at an accelerating voltage of 20 kV. Transmission electron microscopy (TEM) and high-resolution transmission electron microscopy (HRTEM) analyses were made with a JEM-2200F (Cs-corrected TEM) electron microscope with an accelerating voltage of 200 kV. Thermogravimetric analysis (TGA) was performed on a Seiko thermogravimetric/differential thermal analyzer-6300 by heating the samples at 5 °C min^{-1} to 800 °C in a nitrogen atmosphere. Solid-state ^{13}C cross-polarization magic angle spin nuclear magnetic resonance (CP-MAS NMR) measurements were performed on a Bruker Avance III 400 spectrometer at 150.877 MHz, and 1024 scans were signal averaged.

Gas adsorption measurements were carried out using a Belsorp mini II (Micromeritics, Japan) device. Before each measurement, the weighed sample was heat treated at 150 °C in vacuum for 16 h. Brunauer–Emmett–Teller (BET) surface area was investigated by N_2 adsorption–desorption isotherms measured at 77 K. Pore size distributions were calculated using nonlocal density functional theory. Total pore volume was determined from N_2 adsorption–desorption isotherms at relative pressure P/P_0 = 0.97. CO_2, CH_4, and N_2 storage adsorption isotherms were measured at 273 and 298 K and up to 1 atm. An ice-water bath and water baths equipped with a temperature sensor were used to control the temperature at 273 and 298 K.

Materials and Methods. All chemicals were purchased from local suppliers and used without purification: iron(III) chloride (Alfa Aesar, 98%), dibenzofuran (Alfa Aesar, 98%), dibenzothiophene (Alfa Aesar, 98%), carbazole (Aldrich, 98%), dimethoxymethane (Alfa Aesar, 98%), indole (Aldrich, 99%), benzofuran (Alfa Aesar, 98%), benzothiophene (Alfa Aesar, 98%), 1,2-dichloroethane (Aldrich, 99%), methanol (Aldrich, 99%), hydrochloric acid (Aldrich, 35%), and ether (Aldrich, 99%). High purity gases were used for the adsorption measurements (N_2: 99.999%), (H_2: 99.999%), (CH_4: 99.5%), and (CO_2: 99.5%).

Synthesis of Microporous Polymeric Networks. Indole (IN), benzothiophene (BT), benzofuran (BF), carbazole (CBZ), dibenzofuran (DBF), and dibenzothiophene (DBT) were selected as monomers for the synthesis of porous networks. The reaction of DMM with the different monomers was carried out in 1,2-dichloroethane. Briefly, IN (17.07 mM, 2.0 g) was dissolved in 30 mL of anhydrous CH_2Cl_2 in a two-necked flask equipped with a condenser. To this solution, DMM (51.21 mM, 4.52 mL) and $FeCl_3$ (51.21 mM, 8.32 g) were added under nitrogen environment. The resulting reaction mixture was heated to 80 °C for 18 h at constant stirring. After cooling to room temperature, the solid product was collected by filtration and repeatedly washed with methanol, concentrated HCl, distilled water, and methanol to remove the unused monomer and catalyst. The product was further purified by Soxhlet extraction in methanol for 24 h and subsequently washed with ether before drying at 90 °C for 24 h. Similarly, for the BT and BF reactions, the mole ratio among the monomer, DMM, and iron(III) chloride was set as 1:3:3. For the reactions of CBZ, DBF, and DBT, the mole ratio among the monomer, DMM, and iron(III) chloride was set as 1:2:2 to obtain maximum porosity.

RESULTS AND DISCUSSION

The FC alkylation of CBZ, DBF, and DBT has been extensively studied.[25−27] It has been shown that in the case of DBF and DBT the alkylating electrophile adds at the positions 2 and 8,[25,26] and CBZ undergoes electrophilic addition at the positions 3 and 6.[27] On the other hand, IN undergoes electrophilic aromatic substitution primarily at position 3 and BF primarily at position 2, while BT has almost equal probability at positions 2 and 3.[28] All these monomers react to form knitting polymers, where chains of these polymers grow through linking with the methylene group of DMM and at the same time this group connects (cross-links) at random positions with aromatic rings of parallel chains of polymers to develop a porous three-dimensional network (Figure 1a). The only byproduct of this reaction is methanol which can be easily removed from the polymer. The reactions of all monomers were carried out in the presence of excess of anhydrous CH_2Cl_2 solvent, which facilitated in developing cross-linking in polymeric nuclei resulting in isolated microporous polymers. Despite the excess washing, all polymer networks exhibited yields in slight excess of 100% which was attributed to trapped catalyst or solvent within the pore structure. All obtained samples were colored ranging from pale yellow to dark brown. Owing to the presence of extensive hyper-cross-linking, these polymers were found to be insoluble in most organic solvents, which simplifies the purification and activation steps. In addition to this, all the polymers were found to be chemically stable even on exposure to dilute solutions of NaOH and HCl. The morphology and crystalline nature of all polymeric networks were investigated by FESEM, TEM, HRTEM, and XRD. The FESEM images (Figure 1b) suggest the formation of solid spheres of submicrometer dimensions for DBT and aggregated particles for CBZ, BT, and BF. Both DBF and IN consist of aggregated particles with long fibrils. TEM images (Figure S1, (left), Supporting Information) further give support to FESEM results, while HRTEM images (Figure S1 (right), Supporting Information) show that these materials are amorphous in nature. As expected, in all cases the XRD data (Figure S2, Supporting Information) do not show any characteristic peak, which strongly confirms the amorphous and noncrystalline nature of the polymer networks.

FTIR spectra were collected for all the materials to investigate the functional groups of these polymers. The presence of bands around 1600−1660 and 3000 cm^{-1} in the FTIR spectra of the samples correspond to the C=C (stretching) vibration and C−H vibration (stretching) in the heteroatomic aromatic ring, respectively (Figure S3, Supporting Information). The characteristic bands at about 860, 1490, and 1190 cm^{-1} are assigned to the stretching vibration of the C−S−

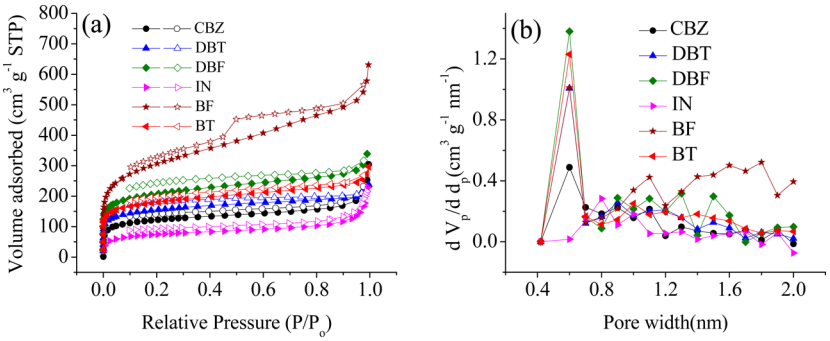

Figure 2. (a) N_2 adsorption–desorption isotherms and (b) pore size distribution for the polymeric networks.

Table 1. Textural Properties of the Polymers

polymer	SA_{BET}[a] (m^2 g^{-1})	V_t[b] (cm^3 g^{-1})	$V_{0.1}$[c] (cm^3 g^{-1})	$\%V_{0.1}/V_t$	PD_{BET}[d] (nm)	PD_{MP}[e] (nm)
CBZ	391	0.40	0.196	49	4.09	0.6
DBT	493	0.344	0.276	80	2.79	0.6
DBF	661	0.523	0.369	71	3.17	0.6
IN	243	0.336	0.104	31	5.52	0.8
BT	571	0.433	0.319	74	3.03	0.6
BF	1022	0.917	0.589	64	3.58	0.6

[a]Specific surface area calculated from the nitrogen adsorption isotherm using the BET method. [b]Total pore volume at P/P_0 = 0.995. [c]Micropore volume. [d]Average pore diameter. [e]Micropore diameter.

C, C–N–C, and C–O–C moieties, respectively. EDX analysis of the polymers was performed to evaluate the purity of the polymeric phase. Only four elements (C, N, S, and O) were detected, which indicates the absence of impurities, specifically the $FeCl_3$ catalyst in the resulting polymers (Figure S4, Supporting Information). Solid-state ^{13}C CP-MAS NMR spectroscopy was used to study the structure of the polymers. In all the materials, peaks at 110–130 ppm were ascribed to the various C atoms in the fused aromatic systems, while the peak below 40 ppm can be assigned to the methylene carbon of the linker. The characteristic peaks at about 155, 138, and 139 ppm correspond to the C atom(s) at the bridge position next to N, S, and O containing moieties, respectively (Figure S5, Supporting Information). Thermal gravimetric analysis shows that all polymeric networks are relatively stable up to 370 °C (Figure S6, Supporting Information). The initial small weight loss (~7%) below 100 °C may correspond to the release of entrapped solvent in the micropores. DBF, DBT, and BT retain more than 50% of their mass at temperatures above 800 °C, while CBZ, IN, and BF lose ~75% of their mass at 800 °C. The least thermal stability is noted for the N containing polymers (CBZ and IN), which agrees with similar trends observed in other reported polymers.[20,29] It is worth mentioning that high thermal stabilities of these polymers are beneficial when considering their potential in postcombustion processes and CO_2 scrubbing operations which occur at higher temperatures.

N_2 adsorption–desorption isotherm measurements at 77 K were utilized to investigate the porous properties of the microporous polymeric networks. Figure 2a shows the N_2 adsorption–desorption isotherms for the resulting polymers. An initial sharp uptake at low relative pressure (P/P_0 = 0–0.1) and a flat uptake at higher relative pressure beyond 0.1 indicate a permanent microporous nature and significant microporous character in the resulting polymers, respectively. According to the IUPAC classification,[30] DBT, DBF, and BT networks exhibited a type I isotherm, while CBZ, IN, and BF networks displayed type I isotherms with mixed type IV character at higher relative pressures. The presence of a small hysteresis in the N_2 desorption curve of the BF strongly suggests a partial mesoporous character, while DBF, DBT, BT, and DBT have mild capillary condensation over P/P_0 of 0.9–0.95. In microporous polymers, this behavior is usually related to interstitial voids within the polymer powder and to the swelling effects of the polymer network while coming in contact with the adsorbate gas.[31] The textural properties of the polymers are summarized in Table 1. BF shows the highest BET specific surface area (SSA) of 1022 m^2 g^{-1}, followed by DBF (661 m^2 g^{-1}), BT (571 m^2 g^{-1}), DBT (493 m^2 g^{-1}), CBZ (391 m^2 g^{-1}), and IN (243 m^2 g^{-1}). The surface area values obtained are slightly lower than many MOPs but still lie in the range of other microporous materials. The average pore size in the micropore region and pore volume was calculated using nonlocal density functional theory. BF shows the largest micropore volume (0.589 cm^3 g^{-1}) of all the polymer networks, followed by DBF (0.369 cm^3 g^{-1}), BT (0.319 cm^3 g^{-1}), DBT (0.276 cm^3 g^{-1}), CBZ (0.196 cm^3 g^{-1}), and IN (0.104 cm^3 g^{-1}). The degree of microporosity in the material was determined by calculating the ratio of micropore volume to the total pore volume ($V_{0.1}/V_t$) (see Table 1). Pore size distributions (PSDs) of the polymers are shown in Figure 2b, and it is clear that the 0.6 nm pore size is dominant in all polymers except IN which shows a dominant pore size of 0.8 nm. These PSD curves are in good agreement with the shape of the nitrogen isotherms (Figure 2a) which provides further strong evidence that all the polymers were predominantly (more than 50%) microporous in nature. It is well-known that knitting of a small aromatic molecular system leads to high SSA materials.[32] In the same way, our materials aromatic systems with two rings (BF, BT) have higher SSA and micropore volume than the aromatic systems with three rings (DBF, DBT). A reverse trend is observed in the case of CBZ and IN, which may be associated with the versatility of the reaction that produces a wide range of possible structural building blocks as well as to the high reactivity of these species.[32] Collectively, oxygen containing polymers display the

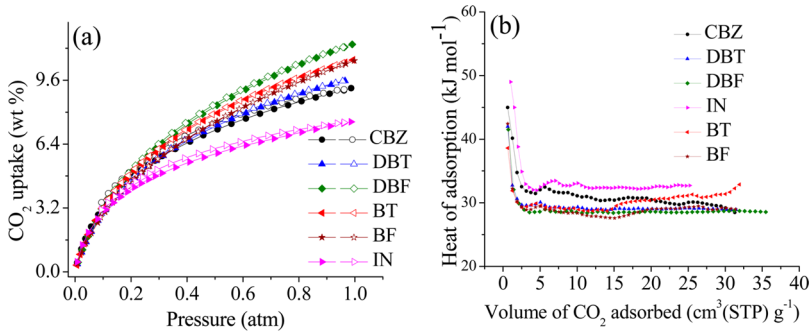

Figure 3. (a) CO_2 adsorption (closed)/desorption (open) isotherms at 273 K and (b) isosteric heat of adsorption of CO_2 for the polymers.

Table 2. Summarized Results of Gas Selectivity and Isosteric Heat of Adsorption for the Polymers

	CO_2/N_2		CO_2/CH_4		CH_4/N_2			
polymer	273 K	298 K	273 K	298 K	273 K	298 K	[a]CO_2 Q_{st}	[a]CH_4 Q_{st}
CBZ	100	76	13.2	13.0	7.5	5.8	45.0	23.0
DBT	86	80	10.7	10.6	8.0	7.6	41.9	30.3
DBF	80	63	11.6	10.2	6.8	6.2	41.5	25.7
IN	65	66	15	15.3	4.3	4.3	49.0	21.3
BT	51	49	12.6	12.4	4.0	4.0	38.6	28.4
BF	43	41	14.9	13.0	2.9	3.1	42.4	20.7

[a]Isosteric heat of adsorption (zero coverage) measured in kJ mol^{-1}.

highest SSA and micropore volume followed by sulfur and nitrogen based polymers.

The microporous nature and the moderately high surface area of these polymers motivated us to study their gas sorption properties. The adsorption properties of the polymeric networks were investigated by using CH_4, N_2, and CO_2 as probe molecules. CO_2 isotherms at 273 K were measured for all polymers and are shown in Figure 3a. Of all the polymers studied, DBF displayed remarkably high CO_2 uptake (11.4 wt %). BT and BF showed an equivalent CO_2 storage capacity (10.2 wt %). DBT, CBZ, and IN captured 9.7, 9.2, and 7.5 wt % CO_2, respectively. Interestingly, these CO_2 uptake values are not only significantly higher than many microporous materials with a similar specific surface area but also comparable to the reported large surface area of porous aromatic frameworks, PAF-1 (9.1 wt %, SSA = 5600 m^2 g^{-1}),[19] PON-1 (10.8 wt %, SSA = 1400 m^2 g^{-1}),[20] and TPI-1 (10.7 wt %, SSA = 809 m^2 g^{-1}).[33] Moreover, these polymers outperform the commercially available BPL carbon which displays a CO_2 adsorption capacity of 9.15 wt %. A comparison of CO_2 uptake by these polymers with other materials is shown in Table S1 (Supporting Information). The average pore diameter of CBZ (4.09 nm) and IN networks (5.52 nm) is larger than that of BF (3.58 nm), DBF (3.17 nm), BT (3.03 nm), and DBT (2.79), which translates into these two polymeric networks having the smallest gas storage capacity of those synthesized. On the other hand, the SSA of BF is about twice the SSA of BT, but both of them have equal CO_2 storage capacity which clearly represents that SSA is not the only dominant factor in CO_2 uptake. As a general statement we can say that the polymer networks with large specific surface area and micropore volume have a larger CO_2 adsorption capacity. This statement however does not hold true for BF that does not show a large CO_2 uptake even after fulfilling these criteria, which is believed to be due to the presence of a relatively larger mesoporous character. The CO_2 adsorption capacity at 298 K follows the same trend as observed at 273 K for all polymers except BT and BF (see Table S2, Supporting Information). This significant affiliation of polymers toward CO_2 is mainly attributed to the presence of a lone pair of electrons on the heteroatoms, which offers dipole−dipole interaction sites, resulting in enhanced CO_2 adsorption properties. The isosteric heat of adsorption (Q_{st}) was also calculated from the CO_2 isotherms measured at 273 and 298 K by using the Clausius−Clapeyron equation to determine the binding affinity of the polymers. From Figure 3b and Table 2, it is clear that the Q_{st} values for zero coverage lie in the very narrow range (49.0−38.6 kJ mol^{-1}) for the polymers. The Q_{st} values obtained for these polymers are relatively larger than many microporous materials, i.e., benzimidazole-linked polymers (BILPs) (26.7−28.8 kJ mol^{-1}),[34] porous electron rich covalent organic nitridic frameworks (PECONFs) (26−34 kJ mol^{-1}),[12] triazine polyimides (TPIs) (35−30 kJ mol^{-1}),[33] and polyimine (PI-1) (34 kJ mol^{-1})[29] but comparable to polyindole fiber (PIF6) (42.7 kJ mol^{-1})[10] and mesoporous silica carbon (IBN9-C1) (44.1 kJ mol^{-1}).[35] These large Q_{st} values are associated with the higher uptake of CO_2 in these materials decorated with heteroatom sites in the low-pressure range. The initially decreasing and then almost stabilizing trend of the Q_{st} with the CO_2 loading suggests that high energy sites are occupied first and then reach a saturation level after a certain amount of CO_2 uptake. In our polymers, the Q_{st} value does not exceed 50 kJ mol^{-1}, which confirms that CO_2 is physically adsorbed in these polymers. Furthermore, the interactions between CO_2 and adsorbent are sufficiently weak which facilitates regeneration of the adsorbent without applying much energy.

The adsorption properties of these materials were further probed by using CH_4 and N_2 at both 273 and 298 K. DBF shows the largest CH_4 uptake (1.47 wt %), followed by BT (1.43 wt %), DBT (1.34 wt %), BF (1.22 wt %), CBZ (1.16 wt %), and IN (0.73 wt %). These values are larger than or comparable to that recently reported for MaSOF-1 (0.98 wt %),[36] salicylbisimine cage compounds (0.98 wt %),[37] mesoPOF-1 (1.49 wt %),[38] BILP-5 (1.77 wt %),[34] BILP-10

dx.doi.org/10.1021/am500728q | ACS Appl. Mater. Interfaces 2014, 6, 7325−7333

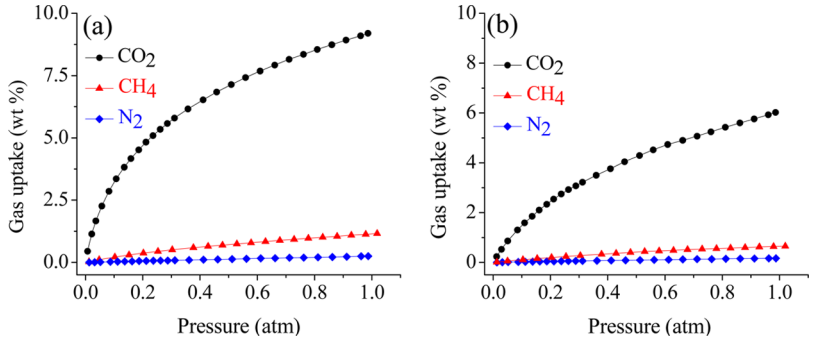

Figure 4. Selective gas adsorption for CBZ at (a) 273 K and (b) 298 K.

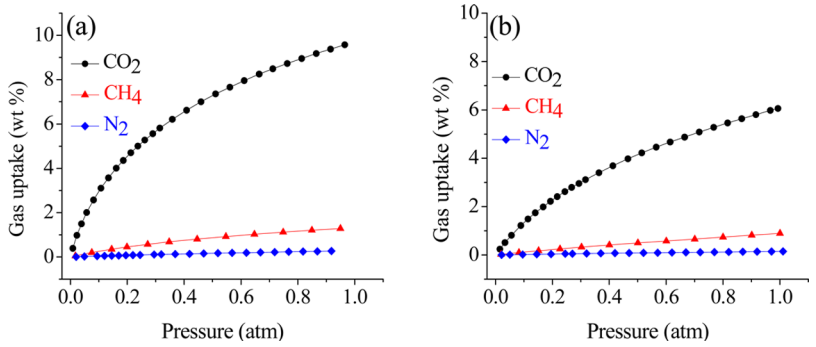

Figure 5. Selective gas adsorption for DBT at (a) 273 K and (b) 298 K.

(1.61 wt %),[39] and CC2 (1.82 wt %)[14] materials. According to the textural properties of the polymers, CH_4 adsorption follows the same sequence as described for CO_2. The Q_{st} of CH_4 was calculated by using adsorption data obtained at 273 and 298 K (Figure S7, Supporting Information), which shows that DBT and BT exhibit the largest zero coverage of 30.3 and 28.4 kJ mol^{-1}, respectively. These values are comparable to PECONF-2 (27 kJ mol^{-1})[12] and PECONF-3 (25 kJ mol^{-1}).[12] The smaller Q_{st} values of CH_4 compared to that of CO_2 are due to its nonpolar nature.

In addition to the CO_2 adsorption capacity and reversibility, a high selectivity for CO_2 over N_2 is one of the key requirements for a material to be applied as a CO_2 adsorbent. Selective adsorption of these polymer networks for different gases (CO_2, CH_4, and N_2) was calculated using initial adsorption slope ratios from Henry's law constants for single-component adsorption isotherms at 273 and 298 K and up to 1 atm (see Table 2 and Figure S8, Supporting Information). In the low-pressure range, the interactions between the network and CO_2 play the dominant role for CO_2 uptake. Thus, the amount of CO_2 adsorbed by CBZ and IN (smaller SSA and larger mean pore diameter) is comparable to BT, BF, DBF, and DBT, suggesting that CBZ and IN have a greater affinity toward CO_2. Among six polymers, CBZ exhibits the highest CO_2/N_2 selectivity ratio of 100 at 273 K (Figure 4 and Figure S9, Supporting Information), whereas DBT, DBF, IN, BT, and BF exhibit ratios of 86, 80, 65, 51, and 43, respectively. This comparably large affinity of CBZ and IN for CO_2 may be attributed to the presence of basic nitrogen moieties and a large Q_{st}. The CO_2/N_2 selectivity ratio of CBZ is better than many recently reported materials including NPM (74),[40] COP-3 (64),[41] PECONF-3 (77),[12] BILP-1 (70),[34] MOPA-B1 II (77),[42] and MPI-2 (71).[43] For MOPs, on increasing the temperature the selectivity usually decreases rapidly due to smaller uptake of gases. Interestingly, at 298 K, the synthesized MOPs have shown a negligible small change in CO_2/N_2 selectivity for DBT (80), IN (66), DBF (63), BT (49), and BF (41), which is contrary to previously reported materials where a drastic decrease (>50% in some cases) was observed, i.e., PECONF-3 (77 to 41),[12] BILP-1 (70 to 36),[34] BILP-3 (59 to 31),[34] BILP-6 (63 to 39),[34] COP-3 (64 to 24),[41] etc. This shows that the synthesized MOPs have shown a stable or far smaller change selectivity trend at two temperatures which has never been observed. It should be noted that the CO_2/N_2 selectivity of MOPs is usually reported at 273 K. However, CO_2/N_2 separation at a temperature of 298 K is closer to the actual postcombustion capture conditions. To the best of our knowledge, the selectivity ratio and CO_2 adsorption observed for the DBT material are among the highest reported at 298 K (Figure 5 and Figure S10, Supporting Information) which made this material more promising for the selective adsorption at fossil fuel power plant conditions. In contrast to DBT and CBZ, the DBF polymer has the highest CO_2 uptake but lowest selectivity. In our samples, high selectivity correlates with low CO_2 uptakes, and we observe a clear trade-off between CO_2 uptake and ideal CO_2/N_2 selectivity (Table S1, Supporting Information).[44,45]

Besides CO_2/N_2 selectivity, natural and landfill gas purification also requires CO_2 separation from CH_4. This application not only helps in increasing energy density but also is equally important for preventing pipeline corrosion. The CO_2/CH_4 selectivity follows a different trend than that of CO_2/N_2 (Table 2). At 273 K, IN shows the highest selectivity ratio of ~15.0, while BF, CBZ, BT, DBF, and DBT show ratios of 14.9, 13.2, 12.6, 11.6, and 10.7, respectively. These results are better than many reported materials with CO_2/CH_4 selectivity ratios, i.e., BILP-1 (10),[46] BILP-10 (14),[39] mesoPOF-2 (14),[38] PECONF-4 (12),[12] MOP polystyrene (13),[47] MPI-2 (12),[43]

and ZIF (10).[48] Similar to the CO_2/N_2 case at 298 K, the CO_2/CH_4 selectivity ratios of the synthesized materials almost remain unchanged in contrast to the materials BILP-1 (7),[46] BILP-2 (12),[34] BILP-10 (7),[39] and PECONF-4 (8),[12] where these selectivity ratios decrease by 3−7 units. In either case of the CO_2/N_2 and CO_2/CH_4 selective adsorption at two different temperatures, stable selectivity data have been observed for these materials. The probable reason may be ascribed to the fact that at these temperatures the synthesized materials have proportional uptake of gases. In all samples, the CH_4 uptake was higher than that of N_2 but significantly lower than the CO_2 uptake (Figure S8, Supporting Information). Since the gas solubility coefficient in a polymer is associated with the critical temperature of gas, CH_4 (191 K) and N_2 (126 K), the CH_4 shows a larger adsorption capacity than N_2.[49] For the same reason, the CO_2/CH_4 selectivity ratio is smaller than the CO_2/N_2 selectivity ratio (Table 2). In the case of the CH_4/N_2 selectivity ratio, this value can be up to ∼8 at 273 and 298 K (Table 2). The flue gases from fossil fuel power plants are emitted around room temperature and 1 atm. Prior to release, they are passed through the adsorbent bed where they are selectively adsorbed. Practically, to capture more pure product, it is desirable to show high selectivity at high temperature. Thus, stable selectivity offers adsorption over a wide temperature range, making use of the captured gas (i.e., CO_2 and CH_4) less energy intensive.

To gain more insight into the interactions between the heteroatomic conjugated systems and CO_2 molecule, theoretical calculations were performed to calculate the binding energies. The interactions between six unit systems (Figure 6) and a CO_2 molecule were estimated by using the density

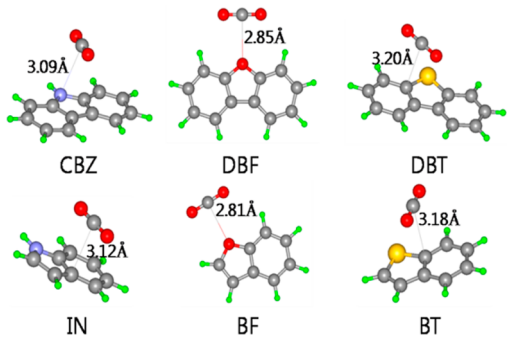

Figure 6. RI-CCSD(T)/aug-cc-pVDZ structures of the six unit systems interacting with the CO_2.

functional theory (DFT) M06-2X method, the spin-component-scaled Møller−Plesset second-order perturbation theory method with the resolution-of-identity approximation (RI-scs-MP2),[50,51] and the coupled cluster theory method with single, double, and perturbative triple excitations with the resolution-of-identity approximation (RI-CCSD(T)) levels of theory. Further details about the calculations were described in the Supporting Information. A good agreement between theory and experiment was observed at the highest calculation level [RI-CCSD(T)]. It is evident that both CBZ and IN (N containing polymeric networks) outperform S and O containing networks. As can be seen in Table 3, the binding energy of IN (18.7 kcal mol^{-1}) and CBZ (17.8 kcal mol^{-1}) is larger than those of the S and O containing moieties DBT (17.4 kcal mol^{-1}), BT (15.9 kcal mol^{-1}), DBF (17.4 kcal mol^{-1}), and BF (15.3 kcal mol^{-1}). The enhanced binding

Table 3. Estimated BEs (kJ/mol) between the Six Unit Systems and CO_2 Molecule

unit system	M06-2X (aug-cc-VDZ)	RI-scs-MP2 (aug-cc-VTZ)	RI-CCSD(T) (aug-cc-pVDZ)
CBZ	14.8	16.9	17.8
DBT	15.3	17.1	17.4
DBF	14.3	15.5	17.7
IN	18.0	17.5	18.4
BT	14.5	15.5	15.9
BF	13.9	13.5	15.3

energies for CBZ and IN are due to the good electron-donor N atom. However, the lone pair electrons of nitrogen are delocalized in the resonance structures. Therefore, the electrostatic interaction is weakened, but the dispersion interaction enhances the binding energy with the CO_2 molecule. While in the DBF and BF each oxygen atom has two lone pairs of electrons. One is delocalized in the resonance structures, and the other is a localized sp^2 lone pair of electrons which interacts electrostatically with the carbon atom of CO_2. The oxygen atoms of CO_2 have weak electrostatic interactions with the close hydrogen atoms of the DBF or BF. Similar to CBZ and IN, the DBT and BT have the π-stacking interactions with the CO_2 molecule due to the large and diffuse S atoms. The larger binding energies that exist between the CO_2 and CBZ and IN indicate more stable and favorable interactions between adsorbent and adsorbate, which translates into an increased adsorption capacity at low pressure and ultimately high selectivity.

CONCLUSIONS

We have prepared six heteroatom-containing microporous organic polymers using an easy, cost-effective Friedel−Crafts reaction. We have shown that the optimized polymer porosities are obtained using 1:2:2 (CBZ, DBT, DBF) and 1:3:3 (IN, BT, BF), molar ratios of monomer:DMM:$FeCl_3$. The BET surface areas of these polymers are in the range 391−1022 $m^2\ g^{-1}$. This simple synthesis approach is helpful in synthesizing polymers that can store large amounts of CO_2. The networks developed by narrow pores and heteroatomic pore surfaces exhibit large adsorption capacities for CO_2 (11.4 wt %, 273 K, and 1 atm). Moreover, it was found that these MOPs offer high selective adsorption for CO_2 over N_2 and CH_4 based on initial slope calculations. These materials not only display high selective adsorption of CO_2/N_2 ∼ 100 and CO_2/CH_4 ∼ 15 at 273 K but also exhibit stable selective adsorption of CO_2/N_2 ∼ 80 and CO_2/CH_4 ∼ 15 at 298 K. The trend of smaller change in selectivity with increase in temperature is in contrast to previously reported materials where a drastic decrease in selectivity was observed. To the best of our knowledge, these CO_2 adsorption and selectivity ratios at 298 K are among the best reported values for any microporous material. Heteroatomic-containing polymeric moieties strongly interact with CO_2, which is clear from the large Q_{st} values (49−38 kJ mol^{-1}). These strong interactions were further confirmed by calculated binding energies using the RI-CCSD(T) method. These heterocyclic microporous polymers offer an opportunity for fine-tuning adsorption and selectivity properties. These factors along with the relatively economical mass-scale manufacturing of these polymers should make them highly competitive in gas storage and selective adsorption applications.

dx.doi.org/10.1021/am500728q | ACS Appl. Mater. Interfaces 2014, 6, 7325−7333

■ ASSOCIATED CONTENT

Supporting Information

Ten figures and two tables, including the TEM images, FTIR and solid-state ^{13}C CP-MAS NMR spectra, X-ray diffraction patterns, TGA data, adsorption selectivities of CO_2 over CH_4 and N_2, isosteric heat of adsorption for CH_4, and theoretical calculations as well. This material is available free of charge via the Internet at http://pubs.acs.org.

■ AUTHOR INFORMATION

Corresponding Author

*Tel.: 82-52-217-5410. Fax: 82-52-217-5419. E-mail: kimks@unist.ac.kr.

Notes

The authors declare no competing financial interest.

■ ACKNOWLEDGMENTS

This research was supported by Basic Science Research Program through the National Research Foundation of Korea (NRF) funded by the Ministry of Education, Science and Technology (2011-0011222), and KISTI (KSC-2012-C3-059). Dr. Nam Suk Lee is gratefully acknowledged for measurement of High Resolution (HR)-TEM, which was performed at the National Institute for Nanomaterials Technology (NINT) at POSTECH, Korea. Dr. Kyungtae Kim is also acknowledged for the thermogravimetric analysis.

■ REFERENCES

(1) Markewitz, P.; Kuckshinrichs, W.; Leitner, W.; Linssen, J.; Zapp, P.; Bongartz, R.; Schreiber, A.; Muller, T. E. Worldwide Innovations in the Development of Carbon Capture Technologies and the Utilization of CO_2. *Energy Environ. Sci.* **2012**, *5*, 7281−7305.

(2) Bohrman, J. A.; Carreon, M. A. Synthesis and CO_2/CH_4 Separation Performance of Bio-MOF-1 Membranes. *Chem. Commun.* **2012**, *48*, 5130−5132.

(3) Saleh, M.; Chandra, V.; Kemp, K. C.; Kim, K. S. Synthesis of N-doped Microporous Carbon via Chemical Activation of Polyindole-modified Graphene Oxide Sheets for Selective Carbon Dioxide Adsorption. *Nanotechnology* **2013**, *24*, 255702.

(4) Chandra, V.; Yu, S. U.; Kim, S. H.; Yoon, Y. S.; Kim, D. Y.; Kwon, A. H.; Meyyappan, M.; Kim, K. S. Highly Selective CO_2 Capture on N-doped Carbon Produced by Chemical Activation of Polypyrrole Functionalized Graphene Sheets. *Chem. Commun.* **2012**, *48*, 735−737.

(5) D'Alessandro, D. M.; Smit, B.; Long, J. R. Carbon Dioxide Capture: Prospects for New Materials. *Angew. Chem., Int. Ed.* **2010**, *49*, 6058−6082.

(6) Kim, D. Y.; Lee, H. M.; Min, S. K.; Hwang, I.; Han, K.; Kim, J. Y.; Kim, K. S. CO_2 Capturing Mechanism in Aqueous Ammonia:NH_3-Driven Decomposition-Recombination Pathway. *J. Phys. Chem. Lett.* **2011**, *2*, 689−694.

(7) Banerjee, R.; Furukawa, H.; Britt, D.; Knobler, C.; O'Keeffe, M.; Yaghi, O. M. Control of Pore Size and Functionality in Isoreticular Zeolitic Imidazolate Frameworks and their Carbon Dioxide Selective Capture Properties. *J. Am. Chem. Soc.* **2011**, *133*, 748−751.

(8) An, J. H.; Geib, S. J.; Rosi, N. L. High and Selective CO_2 Uptake in a Cobalt Adeninate Metal-Organic Framework Exhibiting Pyrimidine and Amino-Decorated Pores. *J. Am. Chem. Soc.* **2010**, *132*, 38−39.

(9) Wood, C. D.; Tan, B.; Trewin, A.; Su, F.; Rosseinsky, M. J.; Bradshaw, D.; Sun, Y.; Zhou, Li.; Cooper, A. I. Microporous Organic Polymers for Methane Storage. *Adv. Mater.* **2008**, *20*, 1916−1921.

(10) Saleh, M.; Tiwari, J. N.; Kemp, K. C.; Yousuf, M.; Kim, K. S. Highly Selective and Stable Carbon Dioxide Uptake in Polyindole-Derived Microporous Carbon Materials. *Environ. Sci. Technol.* **2013**, *47*, 5467−5473.

(11) Islamoglu, T.; Rabbani, M. G.; El-Kaderi, H. M. Impact of Post-Synthesis Modification of Nanoporous Organic Frameworks on Small Gas Uptake and Selective CO_2 Capture. *J. Mater. Chem. A* **2013**, *1*, 10259−10266.

(12) Mohanty, P.; Kull, L. D.; Landskron, K. Porous Covalent Electron-Rich Organonitridic Frameworks as Highly Selective Sorbents for Methane and Carbon Dioxide. *Nat. Commun.* **2011**, *2*, 401−406.

(13) El-Kaderi, H. M.; Hunt, J. R.; Mendoza-Cortes, J. L.; Cote, A. P.; Taylor, R. E.; O'Keeffe, M.; Yaghi, O. M. Designed Synthesis of 3D Covalent Organic Frameworks. *Science* **2007**, *316*, 268−272.

(14) Tozawa, T.; Jones, J. T. A.; Swamy, S. I.; Jiang, S.; Adams, D. J.; Shakespeare, S.; Clowes, R.; Bradshaw, D.; Hasell, T.; Chong, S. Y.; Tang, C.; Thompson, S.; Parker, J.; Trewin, A.; Bacsa, J.; Slawin, A. M. Z.; Steiner, A.; Cooper, A. I. Porous Organic Cages. *Nat. Mater.* **2009**, *8*, 973−978.

(15) Kemp, K. C.; Seema, H.; Saleh, M.; Le, N. H.; Mahesh, K.; Chandra, V.; Kim, K. S. Environmental Applications Using Graphene Composites: Water Remediation and Gas Adsorption. *Nanoscale* **2013**, *5*, 3149−3171.

(16) Cooper, A. I. Conjugated Microporous Polymers. *Adv. Mater.* **2009**, *21*, 1291−1295.

(17) Dawson, R.; Cooper, A. I.; Adams, D. J. Nanoporous Organic Polymer Networks. *Prog. Polym. Sci.* **2012**, *37*, 530−563.

(18) Tsyurupa, M. P.; Davankov, V. A. Hypercrosslinked Polymers: Basic Principle of Preparing the New Class of Polymeric Materials. *React. Funct. Polym.* **2002**, *53*, 193−203.

(19) Ben, T.; Pei, C.; Zhang, D.; Xu, J.; Deng, F.; Jing, X.; Qiu, S. Gas Storage in Porous Aromatic Frameworks (PAFs). *Energy Environ. Sci.* **2011**, *4*, 3991−3999.

(20) Jeon, H. J.; Choi, J. H.; Lee, Y.; Choi, K. M.; Park, J. H.; Kang, J. K. Highly Selective CO_2-Capturing Polymeric Organic Network Structures. *Adv. Energy Mater.* **2012**, *2*, 225−228.

(21) Schmidt, J.; Weber, J.; Epping, J. D.; Antonietti, M.; Thomas, A. Microporous Conjugated Poly(thienylene arylene) Networks. *Adv. Mater.* **2009**, *21*, 702−705.

(22) Rose, M.; Bohlmann, W.; Sabo, M.; Kaskel, S. Element−Organic Frameworks with High Permanent Porosity. *Chem. Commun.* **2008**, 2462−2464.

(23) Germain, J.; Frechet, J. M.; Svec, F. Hypercrosslinked Polyanilines with Nanoporous Structure and High Surface Area: Potential Adsorbents for Hydrogen Storage. *J. Mater. Chem.* **2007**, *17*, 4989−4997.

(24) Germain, J.; Frechet, J. M.; Svec, F. Preparation of Size-Selective Nanoporous Polymer Networks of Aromatic Rings: Potential Adsorbents for Hydrogen Storage. *Chem. Mater.* **2008**, *20*, 7069−7076.

(25) Rao, S. P.; Jones, M. B.; Baltisberger, R. J.; Burger, V. T.; Brown, C. E. Copolymerization of Dibenzofuran and Dichloromethane. *J. Polym. Sci., Polym. Lett. Ed.* **1983**, *21*, 551−558.

(26) Gipstein, E.; Ouano, A. C.; Hewett, W. A. Synthesis and Characterization of Dibenzothiophene-Formaldehyde Copolymers. *Macromolecules* **1972**, *5*, 249−253.

(27) Park, M.; Buck, J. R.; Rizzo, C. J. A Convenient Synthesis of 3,6 Substituted Carbazoles via Nickle Catalyzed Cross-Coupling. *Tetrahedron* **1998**, *54*, 12707−12714.

(28) Sainsbury, M. Heterocyclic Chemistry. *R. Soc. Chem.* **2001**, 97−114.

(29) Laybourn, A.; Dawson, R.; Clowes, R.; Iggo, J. A.; Cooper, A. I.; Khimyak, Y. Z.; Adams, D. J. Branching Out with Aminals: Microporous Organic Polymers from Difunctional Monomers. *Polym. Chem.* **2012**, *3*, 533−537.

(30) Sing, K. S. W.; Everett, D. H.; Haul, R. A. W.; Moscou, L.; Pierotti, R. A.; Rouquerol, J.; Siemieniewska, T. Reporting Physiosorption Data for Gas/Solid Systems with Special Reference to the Determination of Surface Area and Porosity. *Pure Appl. Chem.* **1985**, *57*, 603−619.

(31) Weber, J.; Thomas, A. Toward Stable Interfaces in Conjugated Polymers: Microporous Poly(p-phenylene) and Poly-

(phenyleneethynylene) Based on a Spirobifluorene Building Block. *J. Am. Chem. Soc.* **2008**, *130*, 6334−6335.
(32) Li, B.; Gong, R.; Wang, W.; Huang, X.; Zhang, W.; Li, H.; Hu, C.; Tan, B. A New Strategy to Microporous Polymers: Knitting Rigid Aromatic Building Blocks by External Cross-Linker. *Macromolecules* **2011**, *44*, 2410−2414.
(33) Liebl, M. R.; Senker, J. Microporous Functionalized Triazine-Based Polyimides with High CO_2 Capture Capacity. *Chem. Mater.* **2013**, *25*, 970−980.
(34) Rabbani, M. G.; El-Kaderi, H. M. Synthesis and Characterization of Porous Benzimidazole-Linked Polymers and Their Performance in Small Gas Storage and Selective Uptake. *Chem. Mater.* **2012**, *24*, 1511−1517.
(35) Zhao, Y.; Zhao, L.; Yao, K. X.; Yang, Y.; Zhang, Q.; Han, Y. Novel Porous Carbon Materials with Ultrahigh Nitrogen Contents for Selective CO_2 Capture. *J. Mater. Chem.* **2012**, *22*, 19726−19731.
(36) Mastalerz, M.; Hauswal, H. S.; Stoll, R. Metal-assisted Salphen Organic Frameworks (MaSOFs) with High Surface Areas and Narrow Pore-size Distribution. *Chem. Commun.* **2012**, *48*, 130−132.
(37) Mastalerz, M.; Schneider, M. W.; Oppel, I. M.; Presly, O. A Salicylbisimine Cage Compound with High Surface Area and Selective CO_2/CH_4 Adsorption. *Angew. Chem., Int. Ed.* **2011**, *50*, 1046−1051.
(38) Katsoulidis, A. P.; Kanatzidis, M. G. Mesoporous Hydrophobic Polymeric Organic Frameworks with Bound Surfactants. Selective Adsorption of C_2H_6 versus CH_4. *Chem. Mater.* **2012**, *24*, 471−479.
(39) Rabbani, M. G.; Sekizkardes, A. K.; El-Kadri, O. M.; Kaafarani, B. R.; El-Kaderi, H. M. Pyrene-Directed Growth of Nanoporous Benzimidazole-linked Nanofibers and Their Application to Selective CO_2 Capture and Separation. *J. Mater. Chem.* **2012**, *22*, 25409−25417.
(40) Lewinski, J.; Kaczorowski, T.; Prochowicz, D.; Lipinska, T.; Justyniak, I.; Kaszkur, Z.; Lipkowski, J. Cinchona Alkaloid−Metal Complexes: Noncovalent Porous Material with Unique Gas Separation Properties. *Angew. Chem., Int. Ed.* **2010**, *49*, 7035−7039.
(41) Patel, H. A.; Karadas, F.; Byun, J.; Park, J.; Deniz, E.; Canlier, A.; Jung, Y.; Atilhan, M.; Yavuz, C. T. Highly Stable Nanoporous Sulfur-Bridged Covalent Organic Polymers for Carbon Dioxide Removal. *Adv. Funct. Mater.* **2013**, *23*, 2270−2276.
(42) Xu, C.; Hedin, N. Synthesis of Microporous Organic Polymers with High CO_2-over-N_2 Selectivity and CO_2 Adsorption. *J. Mater. Chem. A* **2013**, *1*, 3406−3414.
(43) Li, G.; Wang, Z. Microporous Polyimides with Uniform Pores for Adsorption and Separation of CO_2 Gas and Organic Vapors. *Macromolecules* **2013**, *46*, 3058−3066.
(44) Dawson, R.; Ratvijitvech, T.; Corker, M.; Laybourn, A.; Khimyak, Y. Z.; Cooper, A. I.; Adams, D. J. Microporous Copolymers for Increased Gas Selectivity. *Polym. Chem.* **2012**, *3*, 2034−2038.
(45) Jiang, S.; Bacsa, J.; Wu, X.; Jones, J. T. A.; Dawson, R.; Trewin, A.; Adams, D. J.; Cooper, A. I. Selective Gas Sorption in a [2 + 3] 'Propeller' Cage Crystal. *Chem. Commun.* **2011**, *47*, 8919−8921.
(46) Rabbani, M. G.; El-Kaderi, H. M. Template-Free Synthesis of a Highly Porous Benzimidazole-Linked Polymer for CO_2 Capture and H_2 Storage. *Chem. Mater.* **2011**, *23*, 1650−1653.
(47) Kaliva, M.; Armatas, G. S.; Vamvakaki, M. Microporous Polystyrene Particles for Selective Carbon Dioxide Capture. *Langmuir* **2012**, *28*, 2690−2695.
(48) Phan, A.; Doonan, C. J.; Uriberomo, F. J.; Knobler, C. B.; O'Keeffe, M.; Yaghi, O. M. Synthesis, Structure, and Carbon Dioxide Capture Properties of Zeolitic Imidazolate Frameworks. *Acc. Chem. Res.* **2010**, *43*, 58−67.
(49) Li, G.; Wang, Z. Naphthalene-Based Microporous Polyimides: Adsorption Behavior of CO_2 and Toxic Organic Vapors and Their Separation from Other Gases. *J. Phys. Chem. C* **2013**, *117*, 24428−24437.
(50) Gerenkamp, M.; Grimme, S. Spin-component Scaled Second-order Møller−Plesset Perturbation Theory for the Calculation of Molecular Geometries and Harmonic Vibrational Frequencies. *Chem. Phys. Lett.* **2004**, *392*, 229−235.
(51) Grimme, S. Improved Second-order Møller−Plesset Perturbation Theory by Separate Scaling of Parallel and Antiparallel-Spin Pair Correlation Energies. *J. Chem. Phys.* **2003**, *118*, 9095−9102.